Scientific Research Publishing

Engineering, 2022, 14, 95-112
https://www.scirp.org/journal/eng
ISSN Online: 1947-394X
ISSN Print: 1947-3931

Effect of Adsorbent/Adsorbate Couple on the Performance of Adsorption Solar Refrigerator

Guy Christian Tubreoumya[1,2], Eloi Salmwendé Tiendrebeogo[1], Oumar Bailou[1], Téré Dabilgou[1,2], Belkacem Zeghmati[2], Alfa Oumar Dissa[1], Jean Koulidiati[1], Antoine Bere[1]

[1]Laboratoire de Physique et de Chimie de l'Environnement (LPCE), Université Joseph Ki Zerbo, Ouagadougou, Burkina Faso
[2]LAboratoire de Mathématiques et Physique (LA.M.P.S), Université de Perpignan Via Domitia (UPVD), Perpignan, France
Email: guytubreoumya@yahoo.fr

How to cite this paper: Tubreoumya, G.C., Tiendrebeogo, E.S., Bailou, O., Dabilgou, T., Zeghmati, B., Dissa, A.O., Koulidiati, J. and Bere, A. (2022) Effect of Adsorbent/Adsorbate Couple on the Performance of Adsorption Solar Refrigerator. *Engineering*, **14**, 95-112.
https://doi.org/10.4236/eng.2022.143009

Received: December 25, 2021
Accepted: March 18, 2022
Published: March 21, 2022

Abstract

This work presents a contribution to the study of the process of cold production by adsorption from solar energy. In this paper, we discuss a comparative study of the operation of a solar adsorption refrigerator using the silica gel-water couple and the zeolite-water couple through dynamic modeling and simulation. The mathematical model representing the evolution of heat and mass transfer at each component of the adsorption solar refrigerator has been developed. It appears from this study that the evolution of the temperature of the two adsorbents (zeolite and silica gel) is quasi-similar throughout the operating cycle. However, the maximum mass of water vapor adsorbed by the silicagel (0.24 kg/kg) is higher than that adsorbed by the zeolite (0.201 kg/kg). In the same way, the mass of water vapor cycled, obtained with the silica-gel-water couple which is 0.14 kg/kg, is higher than that obtained with the zeolite-water couple which is 0.081 kg/kg. Therefore, the amount of cold produced 9.178 MJ and the solar coefficient of performance 0.378 obtained with the solar refrigerator using the silica gel-water couple, are better.

Keywords

Solar Cooling, Adsorption, Zeolite, Silica Gel, Water, Heat and Mass Transfer

1. Introduction

The solar adsorption refrigerators allow to cover the refrigeration needs from the conversion of solar radiation into thermal energy. These adsorption machines represent an interesting alternative because of the good reversibility of the adsorption phenomenon and the simplicity of their manufacture. The technology of cold production by adsorption based on solar energy is very interesting for

countries with a very high irradiation as some regions of Africa, in particular Burkina Faso.

In addition, these adsorption solar refrigeration systems have an ecological advantage, because they use refrigerants that have a low impact on the environment compared to conventional refrigerants such as CFCs (chlorofluorocarbons), HCFCs (hydrochlorofluorocarbons) and HFCs (hydrofluorocarbons). These fluids are harmful to the ozone layer and contribute to the greenhouse effect. Since the Montreal Protocol in 1987, international agreements have called for the reduction of emissions of these refrigerants [1]. Therefore, adsorption solar refrigeration machines represent a promising solution to address both ecological and energy issues.

Indeed, adsorption solar refrigeration machines use refrigerants such as water [2], methanol [3] and ammonia [4]. These fluids are combined with adsorbents such as activated carbon, silica gel, and zeolite to form adsorbent-adsorbate pairs for refrigerator operation.

1.1. Type of Adsorbent-Adsorbate Couple

In sorption refrigeration, the choice of the adsorbent-adsorbate couple is very important. It is made according to the temperature levels of the refrigerating use envisaged (refrigeration, air-conditioning, freezing). Among the couples commonly used for refrigeration, we distinguish:

1.1.1. The Activated Carbon-Methanol Couple

The couple consisting of activated carbon and methanol is the most studied couple in recent research [5] [6] [7]. With methanol, it is possible to produce cold at temperatures below 0˚C. Studies by Mimet, (1991) and Grenier and Pons (1984) showed that the main drawback of this couple is the decomposition of methanol at high temperatures (around 150˚C), which requires working at regeneration temperatures below 120˚C to avoid this situation [8] [9].

1.1.2. Activated Carbon-Ammonia and Zeolite-Ammonia Pairs

They present many advantages, since on the one hand, ammonia supports high regeneration temperatures and on the other hand, ammonia can produce cold at very low temperatures [8]. Studies by Mimet (1991) and Critoph (2002) have shown that ammonia is the most suitable refrigerant for cold production when the adsorbent is activated carbon. Nevertheless, the development of ammonia systems has been confronted on the one hand, with the refusal of the user and on the other hand, with the requirements of the regulation since ammonia is classified as toxic and flammable product [8] [10].

1.1.3. The Silica Gel-Water Couple

This couple has been less studied than the zeolite-water and activated carbon-methanol couples. It is also suitable for refrigeration and air conditioning. Theoretical and experimental studies have been carried out by some authors [11] [12] in order to elucidate its behavior, its operation and its possibility to be used

for the production of cold.

1.1.4. The Zeolite-Water Couple

This couple is very well adapted for air conditioning as well as for refrigeration, but it is not suitable for freezing, because its temperature range is reduced to the interval 0˚C to 10˚C. Therefore, it cannot be used in freezing applications. Water is an "ideal" fluid from the point of view of its toxicity and its environmental footprint. It is also a perfectly safe refrigerant for humans, available and has good thermal properties. This couple has been used by several authors in the field of cold production, including Tchernev (1982), Lu *et al.* (2003), Dahomé and Meunier (1998), Grenier *et al.* (1988) [13] [14] [15] [16].

1.2. Selection Criteria

The most important characteristics of adsorbates are: latent heat, specific volume, saturation pressure, stability with the adsorbent used and environmental impact (Table 1).

Indeed, methanol (CH_3 OH) is a possible gas that is adsorbed by activated carbon. It has been studied and used many times in the last years. However, the decomposition of methanol at temperatures above 150˚C requires precautions for its use in solar applications.

Ammonia has been commonly used for both heating and cooling processes. This fluid is stable over a wide range of temperatures and pressures. It has a high enthalpy of vaporization and a freezing point of −77˚C at atmospheric pressure. Moreover, it is relatively abundant and affordable. However, at high temperatures, ammonia has a very high pressure and, in addition, it is volatile, toxic and corrosive.

Water has the advantage of being stable over a wide range of temperature and pressure, having a high enthalpy of vaporization, being abundant, neutral and non-toxic. However, the pressure of use is very low (below atmospheric pressure). So its implementation requires vacuum technologies. Moreover, its solidification temperature does not allow it to be used for very low temperature applications.

Our study is focused on the adsorption solar refrigerator intended for the conservation of pharmaceutical products in a temperature range between 2˚C and 8˚C. Regarding the temperature range and the environmental challenge, the zeolite-water and silica gel-water couples present better advantages than the others.

Thus, the development of solar adsorption refrigeration machine technology necessarily involves experimental studies on the one hand, and mathematical modeling on the other. The modeling method is not only economical, but also easy to implement in order to simulate the system operation. Therefore, the objective of this work is to model and simulate the operation of the different components of a solar adsorption refrigerator using zeolite-water and silica gel-water couples and to discuss the influence of these types of couples on the performance of the machine.

Table 1. Performance of the solar refrigerator: Influence of the type of adsorbents.

Adsorbent/adsorbate	Silicagel-water	Zeolite-water
Q_f [MJ]	9.178	6.248
COP_s	0.378	0.258

2. Materials and Methods

2.1. Description of the Type of Solar Refrigerator in Our Study

Figure 1 shows the schematic diagram of the prototype refrigerator adopted in our study. This adsorption refrigerator works with the zeolite/water and silica gel/water couples. From the architectural point of view, it is composed of a collector-adsorber, a condenser and an evaporator housed in the refrigeration chamber.

- **The collector-adsorber**

The adsorber-catcher consists of an ordinary single-glazed flat plate collector, resting on a parallelepipedic adsorber with dimensions of 10 cm × 110 cm × 90 cm and composed of two compartments. One of the compartments is filled with adsorbent (zeolite 13X or silicagel) and the other is connected to a pipe which allows to transfer the water vapor towards the condenser or coming from the evaporator. The collector is tilted from the horizontal, by an angle corresponding to the latitude of the place, to allow a better capture of the solar radiation.

- **The condenser**

The condenser is a heat exchanger where the vapour of the refrigerant from the adsorbent bed is liquefied. The air-cooled condenser of our refrigerator is made up of a cylindrical copper tube, 65 cm long, 1 cm thick and 10 cm in diameter. It has copper fins spaced 15 mm apart from each other. Each fin has a square section of 20 cm side and 1 mm thickness. The condenser is positioned in the solar refrigeration system so that the condensate can easily flow by gravity through one of the openings to the evaporator.

- **The evaporator**

The evaporator is the place where the liquid adsorbate vaporizes. It is made of copper tubes of 5 mm thickness and 25 mm internal diameter with a total exchange surface of 0.7 m^2. It has been dimensioned taking into account the mass of water vapor cycled, the exchange surface and the empty space used for the evaporation and circulation of the water vapor. The evaporation of the water leads to the cooling of the refrigeration chamber. To minimize heat loss, the walls of the refrigeration chamber are insulated with a 10 cm thick layer of glass wool.

2.2. Mathematical Formulation

2.2.1. Simplifying Assumptions

Certain assumptions are necessary for an approximate simulation of the system. Thus, in the present study, we assume that:

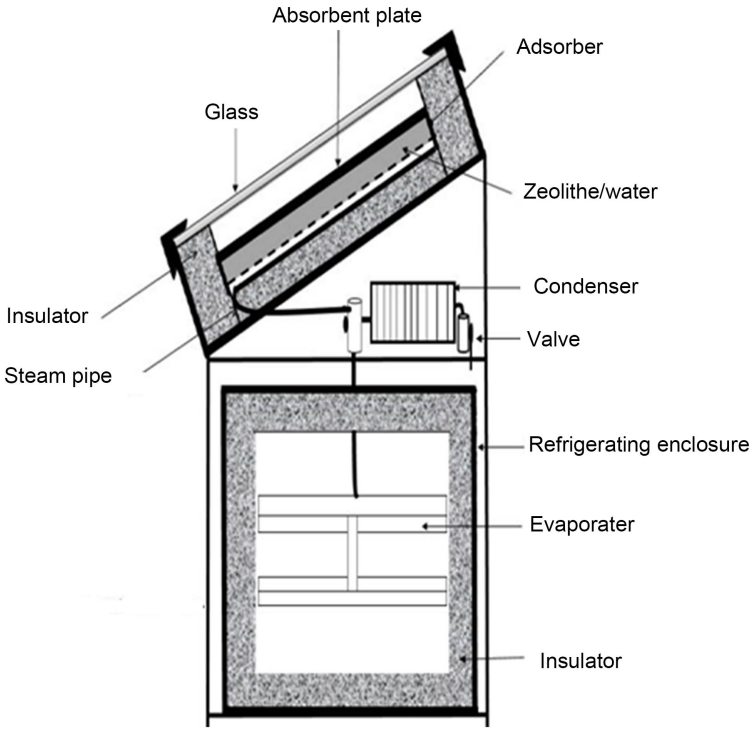

Figure 1. Schematic of the solar adsorption refrigerator.

- the porous material (adsorbent) can be assimilated to a medium with temperature T and equivalent thermal conductivity;
- the heat transfer is unidirectional;
- the convective heat transfer and the pressure losses are negligible in the porous medium;
- the pressure remains constant in the condenser and in the evaporator;
- the total mass of desorbed adsorbate vapor condenses completely;
- the mass transfer resistance is negligible;
- the physical properties of the adsorbent and the metal walls of the adsorber, condenser and evaporator are considered constant.

2.2.2. Modeling of Heat and Mass Transfers in the Solar Refrigerator

The developed model is a so-called "global" model. It takes into account the interaction between the elements that make up the refrigeration plant and allows to highlight the types of coupling existing between them. This model is based on the hypothesis that each element is characterized by quantities supposed to be uniform (nodal method). In our case, these quantities will be the temperature, the pressure and the mass of adsorbed water vapor.

The establishment of the transfer equations is based on the analogy between thermal and electrical transfers. By considering each slice as an entity independent of the others, it is possible to describe the evolution over time of the heat transfers in the solar adsorption refrigeration system. Generally speaking, the instantaneous variation of the energy within a slice (i) of our model is equal to the algebraic sum of the flux densities exchanged within this slice. It is written:

$$m_i Cp_i \frac{\partial T_i}{\partial t} = \sum_i h_{xij} S_{ij} \left(T_j - T_i\right) + \Phi_{ij} \quad (1)$$

j the index of the medium for which T_j is a potential connected to the potential T_i, the heat source or sink (W), the heat transfer coefficient between the media i and j (W/m²K) according to the mode conduction or convection or radiation and the surface of the section considered (m²).

Hereafter, this Equation (1) will be applied to the different components of the adsorption solar refrigerator.

1) Energy balance of heat and material transfers at the collector-adsorber level

- **Energy balance of glass**

The energy balance at the level of the glass cover is reflected in the thermal exchanges between it and the outside air, the vault and the absorbing plate

$$\begin{aligned} m_v Cp_v \frac{\partial T_v}{\partial t} = {} & \alpha_v \cdot G_n \cdot s_v + h_{p-v} \cdot s_v \left(T_p - T_v\right) - h_{cv-v-ext} \cdot s_v \left(T_v - T_{amb}\right) \\ & - h_{r-v-ciel} \cdot s_v \left(T_v - T_{ciel}\right) \end{aligned} \quad (2)$$

T_v is the temperature of the glass, T_p the temperature of the absorber plate and T_{amb} the temperature of the ambient environment.

- **Energy balance of absorber plate**

The heat transfer balance at the absorber plate is written:

$$m_p Cp_p \frac{\partial T_p}{\partial t} = \left(\alpha\tau\right)_{eff} s_p G_n - h_{p-v} s_v \left(T_p - T_v\right) - h_{p-a} s_p \left(T_p - T\right) \quad (3)$$

where T is the equilibrium temperature of the zeolite/water mixture and h_{p-a} the heat transfer coefficient between the absorber plate and this mixture.

- **Energy balance of adsorbent bed**

The energy balance equation for the adsorbent bed can be written as follows:

o During the isosteric heating and desorption phase

$$m_{eq} Cp_{eq} \frac{\partial T}{\partial t} = h_{p-a} \cdot s_p \left(T_p - T\right) + \delta \left(\Delta H_{des} \cdot m_a \cdot \frac{\partial m^{des}}{\partial t} + m_a \cdot Cp_l \left(T - T_{cd}\right) \cdot \frac{\partial m^{des}}{\partial t} \right) \quad (4)$$

o During the isosteric cooling phase and adsorption

$$m_{eq} Cp_{eq} \frac{\partial T}{\partial t} = h_{p-a} \cdot s_p \left(T_p - T\right) + \delta \left(\Delta H_{ads} \cdot m_a \cdot \frac{\partial m^{ads}}{\partial t} - m_a \cdot Cp_l \left(T - T_{ev}\right) \frac{\partial m^{ads}}{\partial t} \right) \quad (5)$$

With:

$\delta = 0$: During isosteric heating and cooling.

$\delta = 1$: During desorption and adsorption.

2) Energy balance of heat and mass transfer at the condenser

During the desorption phase, the condenser is connected to the adsorber. The mass of desorbed water vapor (m_d) from the adsorbent bed enters the condenser where it is cooled and condensed to a liquid state. Thus, the walls of the condenser receive the heat given off by the vapor which in turn cools by convection and radiation to the surrounding environment. Thus the balance equation of

conservation of energy and mass is given by:

$$\begin{aligned}&\left[m_{cd}\cdot Cp_{cd}+m_d\left(t\right)\cdot Cp_l\right]\frac{\partial T_{cd}}{\partial t}\\&=m_a\cdot\frac{\partial m^{des}}{\partial t}\left[L_{cond}\left(P_{cd}\right)+Cp_l\left(T-T_{cd}\right)\right]\\&-h_{r-cd-ciel}\cdot S_{cd}\left(T_{cd}-T_{ciel}\right)-h_{cv-cd-amb}\cdot S_{cd}\left(T_{cd}-T_{amb}\right)\end{aligned}\tag{6}$$

where $m_d\left(t\right)$ represents the total mass of adsorbate vapor desorbed, T_{cd} the temperature of the condenser and L_{cond} the latente heat of condensation.

3) Energy balance of heat and mass transfer at the evaporator

During the evaporation-adsorption period, the evaporator is connected to the collector-adsorber. Thus the partial evaporation of the adsorbate lowers the temperature of the adsorbent bed which continues to adsorb this vapor. The evaporation continues under the combined effect of the heat extracted at the evaporator and the adsorption of the vapors by the adsorbent bed. Thus the heat and mass transfer equation at the evaporator is expressed as:

$$\begin{aligned}&\left[m_{ev}Cp_{ev}+\left(m_d\left(t\right)-\Delta m\cdot m_a\right)Cp_l\right]\frac{\partial T_{ev}}{\partial t}\\&=-m_a\frac{\partial m^{ads}}{\partial t}\left[L_v\left(P_{ev}\right)-Cp_l\left(T-T_{ev}\right)\right]-h_{cv-ev-air}S_{ev}\left(T_{ev}-T_{air}\right)\end{aligned}\tag{7}$$

where T_{ev} is the temperature of the evaporator and L_v the latent heat of vaporization.

2.2.3. Model of Adsorption Kinetics

A thorough examination of these led us to choose the phenomenological model of Dubinin-Astahkov which is best suited to the problem at hand. Thus the equation of the Dubinin-Astahkov model expressing the mass of adsorbate adsorbed on the surface of the adsorbent as a function of temperature (T) and pressure (P) is written:

$$m=w_0\rho_l\left(T\right)\exp\left(-D\left(T\ln\frac{P_s\left(T\right)}{P}\right)^n\right)\tag{8}$$

where $\rho_l\left(T\right)$ is the density of the adsorbate (water), $P_s\left(T\right)$ the saturation pressure, w_0 the maximum adsorption capacity; D and n are constants depending on the adsorbent/adsorbate couple used. Using Antoine's equation giving the saturation pressure:

$$P_s\left(T\right)=1000\cdot\exp\left(16.89-\frac{3803.9}{T-41.68}\right)\tag{9}$$

where T is the temperature in K.

2.2.4. Coefficient of Performance of the System

The solar coefficient of performance (COP_s) of a solar refrigeration machine is defined as the ratio between the amount of cold produced at the evaporator and the total solar energy incident during a full day

$$COP_s = \frac{Q_f}{\int_{t_{sr}}^{t_{ss}} A_s \cdot G_n \cdot \mathrm{d}t} \tag{10}$$

where A_s is the collection area and G_n is the solar flux in W/m^2.

Q_f the amount of cold produced at the evaporator, given by:

$$Q_f = m_a \Delta m \left[L(T_{ev}) - \int_{T_{ev}}^{T_{cd}} Cp_l(T)\mathrm{d}T \right] \tag{11}$$

2.2.5. Determination of Heat Transfer Coefficients

- **The convective transfer coefficient between the glass and the ambient air**

The convective exchange coefficient between the collector glass and the ambient air depends mainly on the wind speed and can be evaluated using the Hottel and Woertz relation

$$h_{cv-v-ext} = 5.67 + 3.86V \tag{12}$$

where V is the wind speed expressed in m/s. This speed must be less than 5 m/s.

- **The convective transfer coefficient between the absorbing plate and the glass**

The convective exchange coefficient between the confined air, the glass and the absorbing plate can be written as follows [17]:

$$h_{cv-p-v} = \frac{Nu \cdot \lambda_{air}}{l} \tag{13}$$

where:

$$Nu = 1 + 1.44\left[1 - \frac{1708(\sin 1.8\theta)^{1.6}}{Ra \cdot \cos\theta}\right]\left[1 - \frac{1708}{Ra \cdot \cos\theta}\right]^* + \left[\left(\frac{Ra \cdot \cos\theta}{5830}\right)^{1/3} - 1\right]^* \tag{14}$$

$$Ra = \frac{g \cdot \beta \cdot \Delta T \cdot l^3 \cdot Pr}{\upsilon^2} \text{ et } 0^\circ \le \theta \le 70^\circ$$

where expressions followed by an asterisk $[\,]^*$ are taken as zero if their value is negative.

R_a is the Rayleigh number, θ the inclination of the collector-adsorber (˚), g = 9.81 m/s^2 the gravitational constant, l the characteristic length; Pr and υ respectively the Prandtl number and the kinematic viscosity of air.

- **The convective heat transfer coefficient between the evaporator walls and the ambient air of the refrigeration chamber**

The natural convective heat transfer coefficient between the air inside the refrigeration chamber and the evaporator walls is determined by the following correlation [18]:

$$Nu = 0.68 + 0.67Ra^{1/4}\left\{1 + \left(\frac{0.492}{Pr}\right)^{9/16}\right\}^{-4/9} \; ; \; 10^{-5} \le Ra \le 10^{12} \tag{15}$$

- **The radiative transfer coefficient between the glass and the absorber plate**

The radiative transfer coefficient between the glass and the absorber plate is given by [19]:

$$h_{r-p-v} = \frac{\sigma}{\frac{1}{\varepsilon_p}+\frac{1}{\varepsilon_v}-1}\left(T_p^2+T_v^2\right)\left(T_p+T_v\right) \tag{16}$$

- **The radiative transfer coefficient between the glass and the sky**

The radiative transfer coefficient between the glass and the sky is determined by the following equation [19]:

$$h_{r-v-ciel} = \sigma\varepsilon_v F_{v-ciel}\left(T_v+T_{ciel}\right)\left(T_v^2+T_{ciel}^2\right); \tag{17}$$

where σ, ε_v and F_{v-ciel} are respectively the emissivity of the glass, the Stefan-Boltzman constant and the form factor between the glass and the sky.

The temperature of the sky is given by the Swinbank formula:

$$T_{ciel} = 0.0552\left(T_{amb}\right)^{1.5} \tag{18}$$

With Tamb the ambient temperature in (K).

- **The radiative heat transfer coefficient between the walls of the condenser and the surrounding environment**

The radiative heat transfer coefficient between the wall of the condenser and the environment in which the condenser is located is given by the relation:

$$h_{r-cd-amb} = \sigma\varepsilon_{cd}\left(T_{cd}+T_{amb}\right)\left(T_{cd}^2+T_{amb}^2\right) \tag{19}$$

where ε_{cd} is the emissivity of the condenser.

3. Mathematical Resolution of the Heat and Mass Transfer Equations

3.1. Initial Conditions

At the initial time, we assume that the temperatures of the adsorber, condenser and evaporator components are equal to the ambient temperature. The pressure in the adsorber is also assumed to be equal to the evaporation pressure corresponding to the saturation pressure at the evaporation temperature.

Thus, for any $t < t_0$, t_0 being the instant from which the collector-adsorber is subjected to the solar flux, we have:

$$T_v\left(t_0\right) = T_p\left(t_0\right) = T_{ev}\left(t_0\right) = T_{cd}\left(t_0\right) = T\left(t_0\right) = T_{amb} \tag{20}$$

$$P\left(t_0\right) = P_{ev} = P_s\left(T_{ev}\right) \tag{21}$$

$$m = m\left(T,P\right) \tag{22}$$

3.2. Model of Discretization of the Equations

The equations have been discretized using an implicit finite difference method. This method, based on the Taylor series development, allows to transform the differential equations into a system of linear equations. The resolution of this

system of equations requires an iterative calculation to determine the physical quantities as a function of the unknown variables at a given time on the one hand, and the variables known at the previous time t on the other hand. The system of equations thus obtained can be presented as a matrix equation with coefficient [A], variable [T] and second member [B].

3.3. Numerical Solution Procedure

The method of solving the system of equations that describes the transient behavior of the model is purely numerical, based on the implicit finite difference method and the iterative method of Gauss Seidel. A computer program written in Fortran language has been developed to model and simulate on the one hand the adsorption-desorption kinetics of the adsorbent/adsorbat couple and, on the other hand, the operation of each element of the refrigerator during one day.

4. Results and Discussion

4.1. Validation by Comparison with Experimental Data

Figure 2 shows the evolution of the pressure in the adsorber-catcher over time obtained by Mayor *et al.*, (2003) [20] and by our model. The results of Mayor *et al.*, (2003) were obtained from experimental data, coming from measurements carried out on the prototype of adsorption solar refrigerator installed in Yverdon-les-Bains (Switzerland) and using the silica gel/water couple. The comparison of these experimental data with our simulation results shows that there is a qualitative agreement between our numerical results and the experimental values obtained by Mayor *et al.* However, between 10 h and 15 h, there are differences between the values of the experimental pressures and those obtained with our numerical code where the maximum deviation is about 18%. These differences would be related to the fact that we considered the condenser and evaporator pressures to be constant.

4.2. Simulation of the Operation of the Solar Adsorption Refrigerator

4.2.1. Temporal Evolution of Solar Radiation and Ambient Temperature

The temporal evolution of global solar radiation and ambient temperature during a typical day in March are shown in Figure 3. It can be seen that the global solar radiation increases from 6am, around the time of sunrise, and reaches a maximum value around 12pm, around noon true sun, then gradually decreases until the end of the day. The maximum value of solar radiation reached, is about 990 W/m^2. The ambient temperature, as for it, evolves according to the activity of the sun and the maximum and minimum values are respectively equal to 313 K and 297 K. These results of the global solar radiation are in the same order of magnitude as those of Ouedraogo I., (2009) [21] who showed that the solar flux of the city of Ouagadougou varies from 500 W/m^2 to 1000 W/m^2 during the greatest hot period.

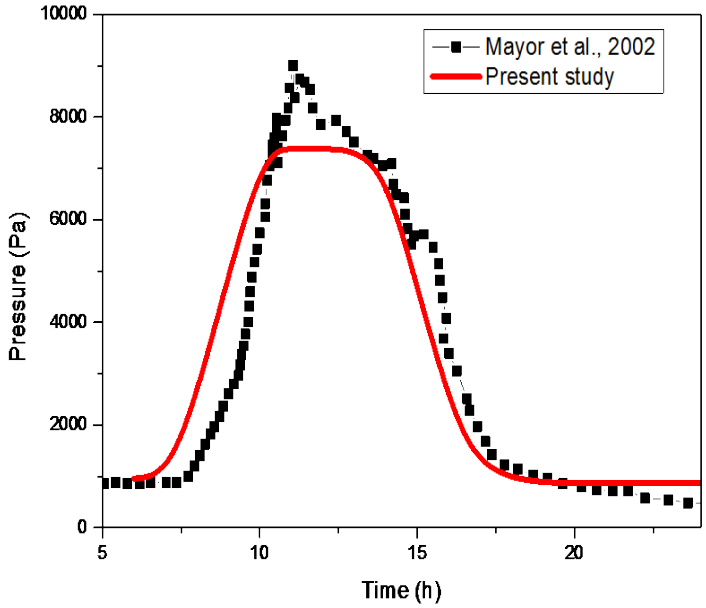

Figure 2. Comparison of the hourly evolution of the pressure.

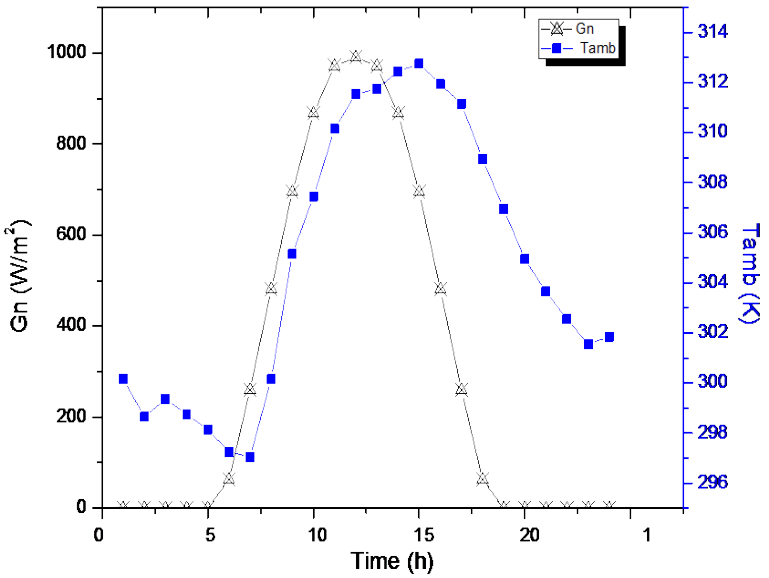

Figure 3. Temporal evolution of ambient temperature and solar irradiance.

4.2.2. Temporal Evolution of the Temperature of the Different Components of the Adsorption Solar Refrigerator

The temporal evolution of the temperatures of the glass, the sorbent plate and the adsorbent bed (zeolite) during the four phases of the cycle are shown in **Figure 4**. At the beginning of the day, the temperatures are identical and equal to the adsorption temperature which, at sunrise, is equal to the ambient temperature. Under the action of the solar flux, the collector-adsorber heats up and the temperatures of its various components increase rapidly over time to reach a maximum value (T_v = 358 K (85˚C), T_p = 396 K (123˚C), T_{zeo} = 395 K (122˚C)) at around 12:00.

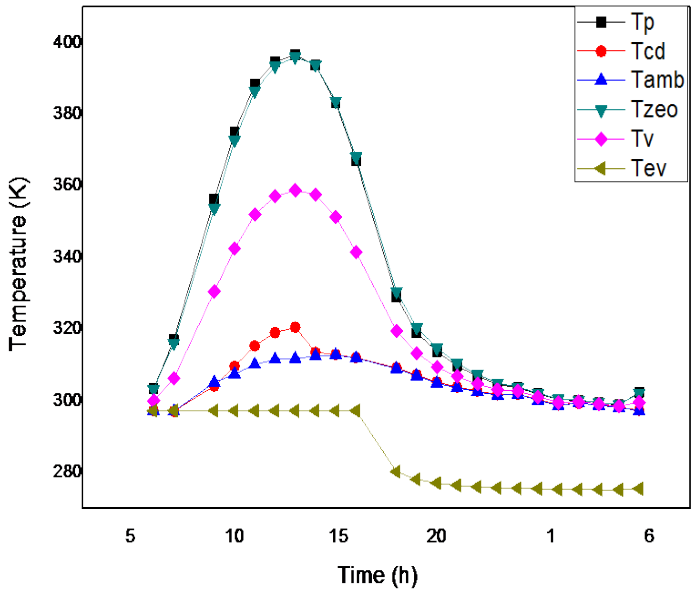

Figure 4. Temporal evolution of the temperature of the differents components of the solar refrigerator.

At the end of the day, the solar flux decreases. This results in a cooling of the adsorber, which starts as soon as the temperature of the adsorbent bed has reached the regeneration temperature. It can be seen that the temperatures of the different compartments of the adsorber decrease up to 300 K (27˚C). This value represents the temperature at which there is no heat exchange between the glass, the plate and the adsorbent bed. The temperature of the adsorbent bed (zeolite) is very close to that of the absorber plate because of the high thermal conductivity of the absorber plate (λ = 400 W/mK) and the almost perfect contact between the zeolite and the plate.

Moreover, the temperature considered as the zeolite temperature (T_{zeo}) is the temperature of the layer that is in contact with the absorber plate. These trends have already been observed by Fadar, (2016), in a numerical study performed on a solar refrigerator using the activated carbon/methanol couple. The author showed that the maximum temperatures of the absorber plate and the adsorbent (activated carbon) reached 355 K (82˚C) and 354 K (81˚C), respectively, for a maximum illuminance of 900 W/m^2 and a maximum ambient temperature of 291 K (18˚C) [22]. Also, Chekirou, (2008), in his numerical study on the solar refrigerator with tubular adsorber using the couple activated carbon /methanol, showed that the values of the temperature of the absorber plate and those of the activated carbon were respectively 370 K (97˚C) and 368 K (95˚C), under an incident radiation of the order of 26.12 MJ/m^2 [23].

The temporal evolution of the condenser temperature during the solar refrigerator operating cycle is shown in **Figure 4**. At the beginning of the cycle, the temperature of the condenser is equal to that of the ambient environment, because at this precise moment of the cycle, the condenser is isolated from the collector-adsorber and does not contain any water vapor. Thus, when the desorp-

tion-condensation phase begins (around 9:00a.m.), the autonomous valve opens and the desorbed water vapor flows into the condenser. The temperature of the condenser rises as a result. At about 1p.m. the condenser temperature reaches its maximum value of about 320 K (47˚C). This increase of the condenser temperature is due to the amount of heat released during the condensation of the water vapor. On the other hand, the decrease of the condenser temperature after 13 h is due on the one hand, to the stop of the desorption process and on the other hand, to the cooling due to the heat transfers by convection and by radiation between the condenser and the ambient environment. It is at this moment that the temperature of the condenser starts to follow that of the ambient temperature and this, for the rest of the day. These same trends were found by Hassan *et al.*, (2011) who conducted numerical studies on the tubular adsorber solar refrigerator and using the activated carbon/methanol pair. The results of this study showed that the maximum temperature reached by the condenser was about 313 K (40˚C), when the maximum solar radiation was 900 W/m^2 [24]. Similarly, Bouzeffour *et al.*, (2016) conducted experimental studies on the operation of the adsorption solar refrigerator using the silica gel/water couple. Their results showed that the maximum temperature that the condenser reached, under incident radiation of 19.423 MJ, was 326 K (53˚C) [25].

The time evolution of the evaporator temperature during the cycle is also shown in **Figure 4**. At the beginning of the day, the refrigeration chamber is closed and the evaporator temperature is equal to the temperature of the ambient air inside the chamber. This temperature remains almost constant during the day due to the good thermal insulation of the refrigeration chamber. At the end of the day, it decreases from about 297 K (24˚) to about 276 K (3˚C). This drop in temperature is due to the evaporation of the condensate (water), which turns into steam and flows towards the adsorbent bed. Thus, the adsorbate takes the heat necessary for its phase change in the refrigeration chamber where the evaporator is located. The evaporator temperature profile obtained with our model, is in agreement with that reported in the work of Umair *et al.*, (2014) where the evaporator temperature decreases and reaches a minimum value of about 280 K (7˚C) [26]. Similarly, Anyanwu *et al.*, (2003) developed a prototype solar refrigerator using activated carbon-methanol pair. This system allows to have temperatures in the evaporator varying from 1˚C to 8˚C and regeneration temperatures between 80˚C and 100˚C [27]. Poyelle *et al.* (1999) also conducted an experimental study on a solar adsorption refrigerator using the zeolite/water couple. These authors showed that the evaporator temperature and the thermal coefficient of performance can reach values of 4˚C and 0.68 respectively [28].

4.3. Influence of the Type of Adsorbent-Adsorbate Couple

Figure 5, **Figure 6** illustrate the temporal evolution of the temperature of the adsorbent and of the mass of water vapor adsorbed during the operation of the solar refrigerator, using successively, the couples zeolite/water and silica gel/water.

It should be noted that the temperature evolution of the two adsorbents is almost similar throughout the operating cycle. However, the maximum mass of water vapor adsorbed by silica gel (0.24 kg/kg) is higher than that adsorbed by zeolite (0.201 kg/kg). Their evolutionary curves decrease progressively to reach respectively minimum values of approximately 0.10 kg/kg and 0.12 kg/kg, before increasing the rest of the cycle. It appears from these results that the mass of water vapor cycled, obtained with the couple silica gel/water which is 0.14 kg/kg, is higher than that obtained with the couple zeolite/water which is 0.081 kg/kg (**Figure 6**).

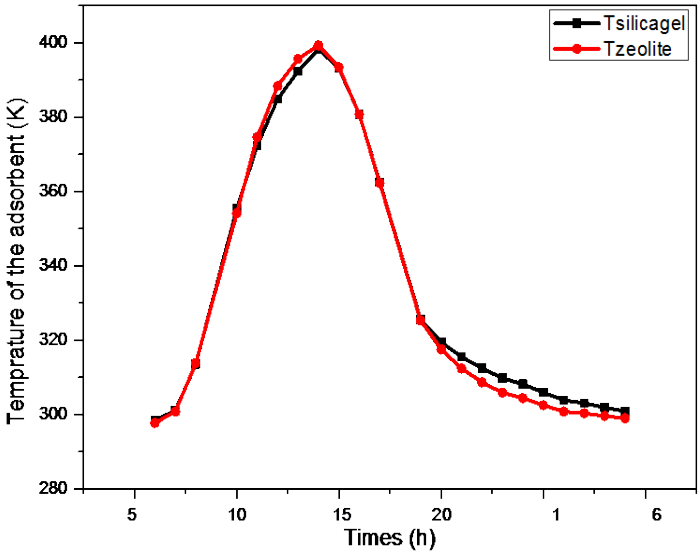

Figure 5. Temporal evolution of the temperature of the adsorbent.

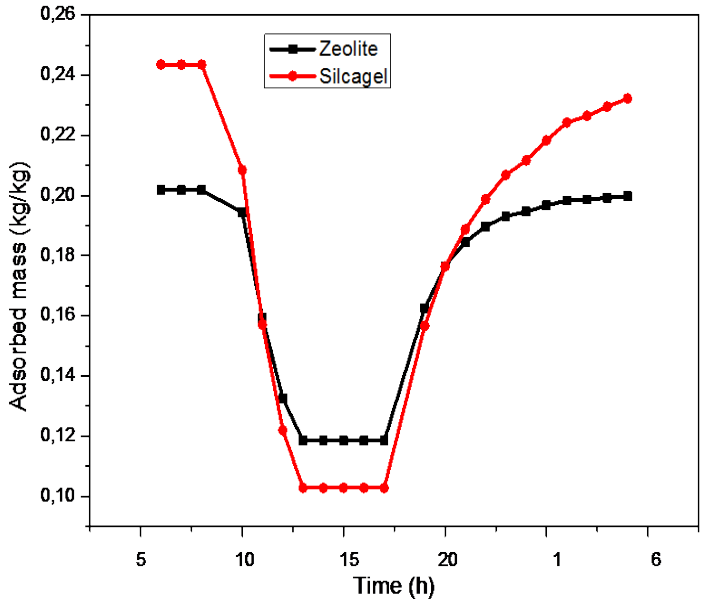

Figure 6. Temporal evolution of the adsorbed water vapor mass.

Table 2. Adsorbent prices.

Adsorbents	Price per kg (Euro)	Price per kg (FCFA)	Supplier reference
Zeolite	2.286	1499.4	Zeolist, (2017)
Silica gel	9.862	6468	Sorbead India, (2017)

NB: the price of zeolite is about 4 times lower than that of silica gel.

Therefore, the amount of cold produced 9.178 MJ and the solar coefficient of performance 0.378 obtained with the solar refrigerator using the silica gel/water couple are higher (**Table 1**). This difference is due to the fact that silica gel and zeolite react differently with water. Indeed, these two adsorbents do not have the same characteristic adsorption properties (specific surface, porosity …) and silica gel is the one with the best ones. These results are in perfect agreement with the work of Allouhi *et al.*, (2015) who conducted a theoretical study of a solar refrigerator using the silica gel/water couple. It emerges from their results that, for an adsorbent mass of 20 kg, a condensation temperature of 25˚C, the COPs reached 0.384 [5]. In 1986, Skoda and Suzuki experimented with an adsorption solar refrigeration machine using the silica gel-water couple. The collector-adsorber used, had a surface of 0.25 m^2, a thickness of 5 cm and a kilogram of silica gel. Its COPs varied between 0.2 and 0.4 [12]. In addition to the most common adsorbent/adsorbate pairs, other pairs have also been studied. In Nigeria, Iloeje *et al.*, (1995) [29] simulated the operation of an adsorption refrigerator using the calcium chloride/ammonia pair. The granular adsorbent is packed in collector tubes of a double glazed solar insolator. The condenser tubes are cooled by water circulating in natural convection. The solar coefficient of performance of the system reaches 0.14.

Beyond the better performance of silica gel, it should be noted that from an economic point of view, the price of zeolite is much lower than that of silica gel (**Table 2**). This makes it an adsorbent widely used in adsorption solar refrigerators.

5. Conclusions

This article aimed, on the one hand, to validate the model of our study and, on the other hand, to analyze the influence of two types of adsorbent-adsorbate couples, namely zeolite-water and silica gel-water couples on the performance of the adsorption solar refrigerator. The results show that the temperature evolution of the two adsorbents (zeolite and silica gel) is almost similar throughout the operating cycle. However, the maximum mass of water vapor adsorbed by silicagel (0.24 kg/kg) is higher than that adsorbed by zeolite (0.201 kg/kg). Similarly, the mass of cycled water vapour obtained with the silica gel-water couple, which is 0.14 kg/kg, is higher than that obtained with the zeolite-water couple which is 0.081 kg/kg. Therefore, the amount of cold produced 9.178 MJ and the solar coefficient of performance 0.378 obtained with the solar refrigerator using the silica gel-water couple, are higher. Thus, with the silica gel-water couple, the

refrigerator presents better performance compared to the zeolite-water couple.

The results found are satisfactory and can constitute a research platform whose goal is to improve the performance of solar systems on the one hand, and on the other hand, to master this process of solar cold production which is still poorly exploited in Burkina Faso.

Acknowledgements

The authors are grateful to the University Agency of the Francophonie (AUF) and the French Embassy (SCAC) for financial support which allowed the realization of this work.

Conflicts of Interest

The authors declare no conflicts of interest regarding the publication of this paper.

References

[1] Anyanwu, E. (2000) Environmental Pollution: Restructuring the Refrigeration Industry as a Way out. *Environment Protection Engineering*, **26**, 17-28.

[2] Wang, D. and Zhang, J. (2009) Design and Performance Prediction of an Adsorption Heat Pump with Multi-Cooling Tubes. *Energy Conversion and Management*, **50**, 1157-1162. https://doi.org/10.1016/j.enconman.2009.01.028

[3] Hassan, H. (2013) Energy Analysis and Performance Evaluation of the Adsorption Refrigeration System. *ISRN Mechanical Engineering*, **2013**, Article ID: 704340. https://doi.org/10.1155/2013/704340

[4] Louajari, M., Mimet, A. and Ouammi, A. (2011) Study of the Effect of Finned Tube Adsorber on the Performance of Solar Driven Adsorption Cooling Machine Using Activated Carbon-Ammonia Pair. *Applied Energy*, **88**, 690-698. https://doi.org/10.1016/j.apenergy.2010.08.032

[5] Allouhi, A., Kousksou, T., Jamil, A., El Rhafiki, T., Mourad, Y. and Zeraouli, Y. (2015) Optimal Working Pairs for Solar Adsorption Cooling Applications. *Energy*, **79**, 235-247. https://doi.org/10.1016/j.energy.2014.11.010

[6] Chekirou, W., Boukheit, W. and Kerbache, T. (2007) Numerical Modeling of Combined Heat and Mass Transfer in a Tubular Adsorber of a Solid Adsorption Solar Refrigerator. *Revue des Energies Renouvelables*, **10**, 367-379.

[7] Fadar, A.E. (2015) Thermal Behavior and Performance Assessment of a Solar Adsorption Cooling System with Finned Adsorber. *Energy*, **83**, 674-684. https://doi.org/10.1016/j.energy.2015.02.074

[8] Mimet, A. (1991) Etude théorique et expérimentale d'une machine frigorifique à adsorption d'ammoniac sur charbon actif. Thèse de Doctorat, FPMs, Mons, Belgique.

[9] Grenier, P. and Pons, M. (1984) Experimental and Theoretical Results on the Use of an Activated Carbon/Methanol Intermittent Cycle for the Application to a Solar Powered Ice Maker. In: Szokolay, S.V., Ed., *Solar World Congress*, Vol. 1. Pergamon Press, Oxford, 500-506.

[10] Critoph, R.E. (2002) Multiple Bed Regenerative Adsorption Cycle Using the Monolithic Carbon-Ammonia Pair. *Applied Thermal Engineering*, **22**, 667-677.

https://doi.org/10.1016/S1359-4311(01)00118-1

[11] Hildbrand, C., Dind, P., Pons, M. and Buchter, F. (2004) A New Solar Powered Adsorption Refrigerator with High Performance. *Solar Energy*, **77**, 311-318. https://doi.org/10.1016/j.solener.2004.05.007

[12] Sakoda, A. and Suzuki, M. (1986) Simultaneous Transport of Heat and Adsorbate in Closed Type Adsorption Cooling System Utilizing Solar Heat. *Journal of Solar Engineering*, **108**, 239-245. https://doi.org/10.1115/1.3268099

[13] Tchernev, D. (1982) Solar Air Conditioning and Refrigeration Systems Utilizing Zeolites. *Proceedings Meetings of IIR Commissions E*1-*E*2, Jerusalem, 22-27 June 1982, 209-215.

[14] Lu, Y.Z., Wang, R.Z., Zhang, M. and Jiangzhou, S. (2003) Adsorption Cold Storage System with Zeolite-Water Working Pair Used for Locomotive Air Conditioning. *Energy Conversion and Management*, **44**, 1733-1743. https://doi.org/10.1016/S0196-8904(02)00169-3

[15] Dahomé, E. and Meunier, F. (1982) Reversible and Irreversible Cycles of a Chemical Heat Pump; Application to the Zeolite 13X/Water System. *Revue Générale de Thermique*, **246**, 483-500.

[16] Grenier, P., Guilleminot, J.J., Meunier, F. and Pons, M. (1988) Solar Powered Solid Adsorption Cold Store. *Journal of Solar Energy Engineering*, **110**, 192-197. https://doi.org/10.1115/1.3268256

[17] Jannot, Y. (2007) Thermique Solaire.

[18] Oleg, G., Martynenko, P. and Khhramtsov, P. (2005) Free-Convective Heat Transfert. Springer-Verlag, Berlin.

[19] Duffie, J.A. and Beckaman, W.A. (1974) Solar Energy Thermal Process. Wiley-Instersciences, Hoboken.

[20] Julien, M., Catherine, H. and Philippe, D. (2002) Domaine Solaire Actif: Construction et test d'un réfrigérateur solaire à adsorption transportable. LESBAT (Laboratoire d'Energétique Solaire et de Physique du Bâtiment) Programme Pilote et Démonstration. Yverdon-les-Bains, Suisse.

[21] Ouedraogo, I. (2009) Modélisation et optimisation d'une toiture bioclimatique pour la climatisation passive d'un habitat type du Burkina Faso. Thèse Doctorat Unique, Université de Ouagadougou, Burkina Faso, 159 p.

[22] Fadar, A.E. (2015) Thermal Behavior and Performance Assessment of a Solar Adsorption Cooling System with Finned Adsorber. *Energy*, **83**, 674-684. https://doi.org/10.1016/j.energy.2015.02.074

[23] Chekirou, W. (2008) Etude et analyse d'une machine frigorifique solaire à adsorption. Thèse de Doctorat, Universite Mentouri, Constantine.

[24] Hassan, H., Mohamad, A. and Bennacer, R. (2011) Simulation of an Adsorption Solar Cooling System. *Energy*, **36**, 530-537. https://doi.org/10.1016/j.energy.2010.10.011

[25] Bouzeffour, F., Khelidj, B. and Tahar, M. (2016) Experimental Investigation of a Solar Adsorption Refrigeration System Working with Silicagel/Water Pair: A Case Study for Bou-Ismail Solar Data. *Solar Energy*, **131**, 165-175. https://doi.org/10.1016/j.solener.2016.02.043

[26] Umair, M., Akisawa, A. and Ueda, Y. (2014) Performance Evaluation of a Solar Adsorption Refrigeration System with a Wing Type Compound Parabolic Concentrator. *Energies*, **7**, 1448-1466. https://doi.org/10.3390/en7031448

[27] Anyanwu, E. (2003) Review of Solid Adsorption Solar Refrigerator I: An Overview

of the Refrigeration Cycle. *Energy Conversion and Management*, **44**, 301-312. https://doi.org/10.1016/S0196-8904(02)00038-9

[28] Poyelle, F., Guilleminot, J. and Meunier, F. (1999) Experimental Tests and Predictive Model of an Adsorptive Air Conditioning Unit. *Industrial & Engineering Chemistry Research*, **38**, 298-309. https://doi.org/10.1021/ie9802008

[29] Iloeje, O., Ndili, A. and Enibe, S. (1995) Computer Simulation of a $CaCl_2$, Solid Adsorption Solar Refrigerator. *Energy*, **20**, 1141-1151. https://doi.org/10.1016/0360-5442(95)00050-Q